Multi-Doppler Resolution Automotive Radar

Oded Bialer and Sammy Kolpinizki
General Motors - Advanced Technical Center Israel

***Abstract*—Automotive radars operate in challenging environments that include objects with similar position and speed as well as objects with diverse positions and velocities. Automated driving requires the radar to discriminate close objects and also to accurately estimate the position of the objects in the field-of-view. Doppler filtering is essential to fulfill this goal. In conventional automotive radars the Doppler processing has a fixed and predetermined filtering integration time and hence a fixed Doppler resolution. However, in this case, setting the Doppler resolution is a tradeoff between high resolution that enables discrimination of close objects and accurate estimation of their position. In this paper we develop a multi-resolution Doppler processing method that resolves this tradeoff. The performance advantages of multi-resolution Doppler processing compared to the conventional fixed Doppler resolution are evaluated in an automotive scenario. It is shown that the multi-resolution Doppler processing attains better discrimination of close objects as well as more accurate position estimation of the objects.**

I. Introduction

The automotive industry is developing vehicles with advanced active safety features as well as autonomous driving features, which will provide more secure driving and reduce the number of accidents on the roads. The automotive radar is a key sensor enabling these features and has a major role advanced technological vehicles of car manufactures.

Driving scenarios may include a relatively large number of crowded different objects with various kinematics, especially in urban environments. For example, the field-of-view (FOV) may include both static objects such as buildings and dynamic objects such as vehicles, bicycle riders and pedestrians moving at various velocities / directions. The automotive radar needs to detect all objects in its FOV and to accurately estimate the position and velocity of each one. These objects may often be in close proximity so that their position difference is below the range and angle resolution of the radar and therefore cannot be separated in position. The implications may be fatal. Having un-separable objects means that their reflections are overlapping, causing offsets in their position estimation [1]. Furthermore, when reflection intensity differences are large (e.g. pedestrian next to a vehicle), the high intensity object may mask the weak intensity object. Fortunately, objects that are in close proximity and cannot be separated in range or azimuth may still be separated by Doppler filtering, as discussed next.

The radar reflection Doppler frequency is given by

$$f_d = 2f_c\frac{v}{c}\cos(\theta), \tag{1}$$

where f_c is the carrier frequency, c is the speed of light, and θ is the angle between the object relative motion vector and the radial vector pointing from the object to the radar. The Doppler filtering resolution is the smallest Doppler frequency difference between two objects that are at similar positions that can still be separated by Doppler filtering such that the angle and range measurements of both objects are not overlapping one over the other, thus, with high enough Doppler resolution two objects at close proximity will not mask each other. Therefore, high Doppler resolution is essential for the automotive radar. Note that from (1) two targets at close proximity and same speed, v, can still be separated by Doppler since they will have different θ values due to their slightly different angles with respect to the radar.

The Doppler resolution is inversely proportional to the Doppler filtering integration time. Hence, increasing that time enables better separation of close objects. However, the integration time is limited since the objects are moving. Having the integration too long results in inaccuracy of the object position estimation. In conventional automotive radars the Doppler integration time is pre-set to 25-50 msec, resulting in a Doppler resolution of 20-40 Hz [2]-[4]. This fixed integration time is set according to the fastest moving object in the FOV, which may have relative speed of 20-50 m/sec and therefore is moving between 1 to 2.5 meters during the integration time, causing position estimation inaccuracy of about 1-2.5m. This inaccuracy in position by itself is insufficient in some cases, but even more so, a Doppler resolution of 20 Hz cannot enable the separation of close proximity objects that have similar relative speeds, as will be shown in Section IV.

In this paper we develop a multi-resolution Doppler filtering method, and analyze its performance advantage for the automotive radar application. Unlike the conventional approach where the Doppler resolution is fixed and limited by the object with maximal velocity, in the multi-resolution Doppler filtering the Doppler resolution changes with frequency. It will be shown that for automotive radar scenarios, the multi-resolution filtering method attains more accurate position estimation of moving objects as well as significantly better separation between close objects, compared to the conventional Doppler filtering with fixed resolution.

II. System model

The automotive radar system that is considered in this paper is depicted in Fig. 1. The radar has multiple transmit and receive antennas. In the transmitter, a sequence of linear frequency chirps is generated and up-converted to carrier frequency, f_c. The transmitted signal is denoted by $x(t)$ and is given by

$$x(t) = \sum_i p(t - iT_c)sin(2\pi f_c t), \tag{2}$$

ISBN 978-0-9928626-7-1

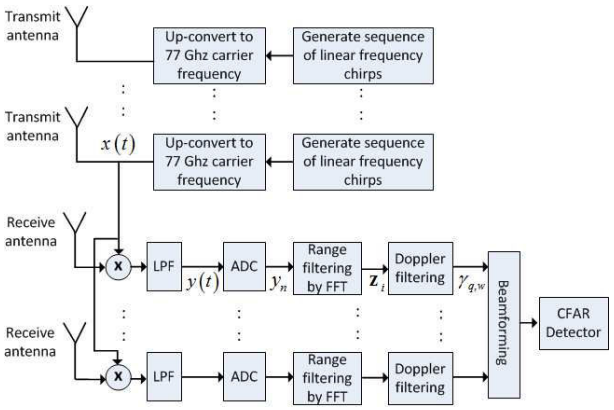

Fig. 1. System model

where T_c is the single chirp duration, and

$$p(t) = \begin{cases} sin(\alpha t^2) & 0 \le t \le T_c \\ 0 & otherwise \end{cases} \quad (3)$$

is the single chirp signal, with linear frequency slope of α. The automotive radar scene includes multiple objects at various ranges, angles and speeds. The received signal at each one of the receive antennas is multiplied with the transmitted signal reference, $x(t)$, and filtered with a low pass filter (LPF) [5]. The resulting base-band signal is denoted by $y(t)$ and is given by

$$y(t) = \sum_m \sum_i s_m(t - iT_c) e^{-j(\phi_m + 2\pi f_m^d t)} + \eta_n, \quad (4)$$

where η_n are the AWGN noise samples, i is the chirp index, m is the reflection index,

$$s_m(t) = \begin{cases} sin(2\pi f_m^r t) & 0 \le t \le T_c \\ 0 & otherwise \end{cases}, \quad (5)$$

where f_m^r is the m-th reflection frequency, which is a result of the propagation delay and thus is a function of the m-th reflection range, and f_m^d is the m-th reflection Doppler frequency. The received base-band samples are denoted by $y_n = y(nT_s)$, where T_s is the sampling interval. The high-level radar processing block diagram presented in Fig. 1 includes the following four steps. First, range filtering is obtained by a FFT on each block of N samples y_n, where $N = T_c/T_s$ is the number of samples in the chirp duration and is assumed to be a power of 2. Let

$$\boldsymbol{z}_i = [\ z_i^0 \quad z_i^1 \quad ... \quad z_i^{N-1}\ ]^T, \quad (6)$$

be the FFT result for the block index i, where the superscript index of the vector elements denotes the range bin index, and the subscript index denotes the FFT block index. Second, Doppler filtering is applied for each range bin separately over multiple vectors $\boldsymbol{z}^i$ [6]-[8]. Let $\gamma_{q,w}$ be the range-Doppler filter output for the q range bin index and the w Doppler bin index. Third, Beamforming is applied on the array response per each range Doppler filtered output, $\gamma_{q,w}$, resulting in a reflection intensity image with dimensions of range, Doppler and angle. Then in the fourth step, the objects are detected by running a constant false alarm detection algorithm (CFAR) [9]-[10] over the radar image. The objects range, Doppler and angle are estimated by the peaks in the radar reflection intensity image.

III. Multi-resolution Doppler filtering

Next, we derive a multi-resolution Doppler filtering algorithm. Unlike the conventional approach, where all Doppler frequencies are filtered with the same integration time, in the multi-resolution approach each Doppler frequency has a different integration time. High speed objects are changing position rapidly and require a short integration time to accurately estimate their position and boundaries. Having a too large integration time for fast moving objects results in smear of the target's position. On the other hand, slow speed objects are changing position slowly and hence can be filtered with a longer integration time than faster ones. By realizing that the high speed objects have high Doppler frequencies while the low speed objects have low Doppler frequencies, we propose to have an integration time that is inversely proportional to the Doppler frequency. Thus the integration time increases as the Doppler frequency is lower. In the multi-resolution Doppler filtering, the Doppler spectrum is divided into K frequency bands (K bins), and a Discrete Fourier Transform (DFT) is applied to each bin with a different pre-configured integration time. The w-th Doppler DFT bin calculated for the q-th range bin is given by

$$\gamma_{q,w} = \sum_{n=0}^{\mu_w - 1} z_n^q e^{-j2\pi \frac{nw}{K}}, \quad (7)$$

where $\mu_w = T_f/T_c$ is the integration samples for the w Doppler frequency bin index (assuming that μ_w is an integer), T_f is the integration time and T_c is the chirp duration. We note that in the conventional automotive radar the Doppler filtering is performed by FFT of the sequence $z_0^q, z_1^q, ..., z_{P-1}^q$ (assuming P is a power of 2). In this case, the number of integration samples, P, are fixed for all the Doppler frequencies and thus the Doppler resolution is the same for all frequencies. In the multi-resolution Doppler filtering the integration times per each Doppler frequency are pre-configured, their proper setting is essential and is discussed next. In order for the automotive radar to accurately estimate the objects position and boundaries the integration time needs to be set such that the dynamic vehicle position does not change significantly during the integration time. Denote by D the maximal tolerated distance change of the object within the integration time, and let v_r be the object speed projected onto the radial direction (the vector pointing from the object to the radar). Therefore, we propose to set the Doppler integration time as

$$T_d = \frac{D}{v_r}. \quad (8)$$

The Doppler frequency is given by

$$f_d = 2 f_c v_r / c, \quad (9)$$

where f_c is the carrier frequency, and c is the speed of light. By substituting (9) into (8) we obtain that the integration time

ISBN 978-0-9928626-7-1 © EURASIP 2017

for Doppler frequency f_d is given by

$$T_f = \frac{2Df_c}{f_d c}. \quad (10)$$

As expected the Doppler filter integration time is inversely proportional to the Doppler frequency. In Fig. 2 we plot the integration time vs. Doppler frequency according to (10) for the automotive radar application, where $f_c = 77Ghz$, the maximal relative speed is 300 kph and $D = 1m$. The integration time is truncated to 500 msec at low Doppler frequencies in order to limit the delay in target detection. For comparison, the 50 msec fixed integration time used for conventional automotive radar Doppler filtering is also plotted in the the dashed red line. Fig. 3 presents the Doppler resolution given by $1/T_f$, which correspond to the integration times in Fig. 2. The Doppler resolution is a measure of the Doppler separability of close objects. The blue plot is the multi-Doppler resolution as a function of the frequency, and the red dashed plot is the conventional fixed Doppler resolution of 20 Hz. It is seen that the multi-resolution method can separate slow speed objects that have small Doppler difference of 5 Hz, while for objects with high speed the Doppler resolution reduces to few tenths of Hz, and by that enabling accurate positioning of the moving object with small positioning offset.

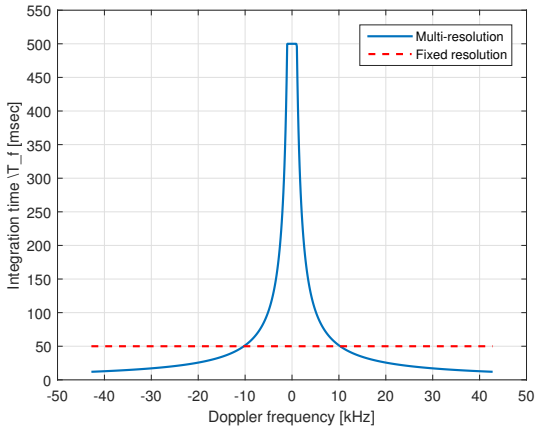

Fig. 2. Integration time vs. Doppler frequency

IV. Results and Discussion

We evaluated the performance of the proposed method with a 77Ghz automotive radar high fidelity ray tracing simulation. The complex surface of vehicles and motorcycle were simulated by many small polygons of size $5cm \times 5cm$. The simulated radar had linear frequency modulation (LFM) transmission, 1Ghz bandwidth, chirp duration of 32 usec, 1 TX antenna and 8 RX antennas at a standard ($\lambda/2$) uniform linear array layout (3dB angular beamwidth of approximately 14°).

Fig. 4 shows a bird-eye view of the simulated scene. It includes the host vehicle 'D' with a radar mounted on its front, a motorcycle in the same lane of the host vehicle marked by 'A', another vehicle in the adjacent lane marked as 'B', and an incoming vehicle marked by 'C. In addition the approximated

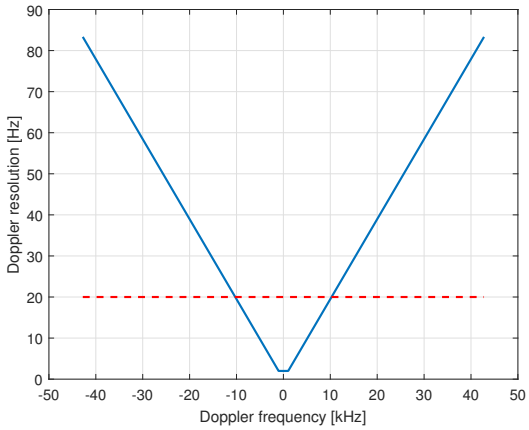

Fig. 3. Doppler resolution vs. Doppler frequency

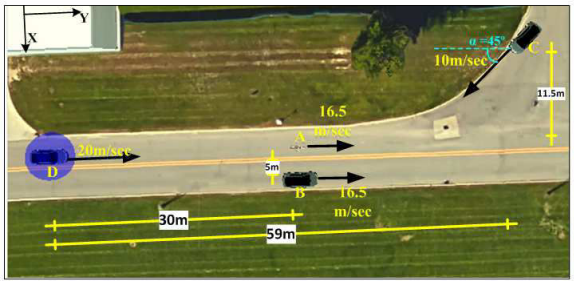

Fig. 4. Bird-eye view of tested scene. Objects, distances and velocities direction and magnitude are marked on the figure. Test radar mounted on front bumper of vehicle 'D'.

velocity vectors, and the relative distances between 'A', 'B', 'C' and 'D' are also marked on the figure. In the test scene the relative velocity between 'D' and 'A' as well as the relative velocity between 'D' and 'B' is slow compared to the relative velocity between 'D' and 'C'.

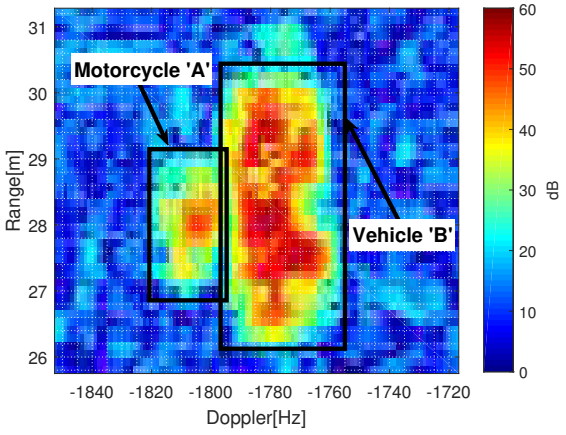

Fig. 5. Range-Doppler spectrum obtained for integration time of 300msec, zoomed in on Motorcycle 'A' and Vehicle 'B' bins.

Figs. 5-7 show the results obtained for processing the samples with 300 msec Doppler processing integration time. Fig. 5 shows a segment of the range-Doppler spectrum focused around the motorcycle 'A' and vehicle 'B'. The geometry

ISBN 978-0-9928626-7-1 © EURASIP 2017

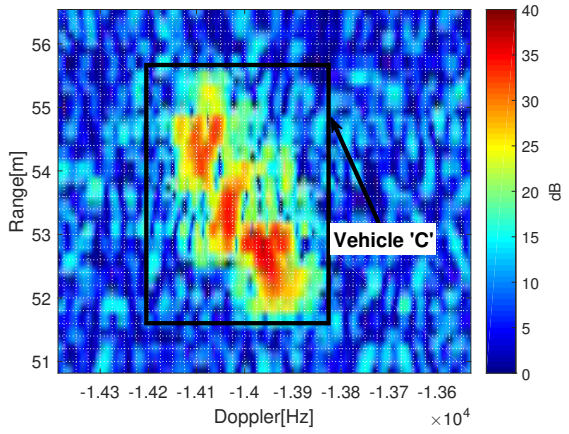

Fig. 6. Range-Doppler spectrum obtained for integration time of 300msec, zoomed in on vehicle 'C bins.

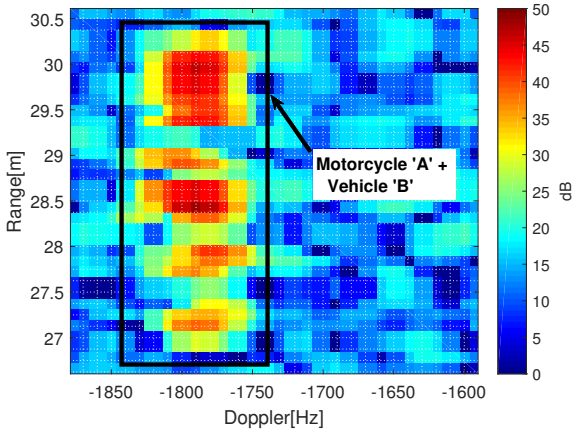

Fig. 8. Range-Doppler spectrum obtained for integration time of 50msec, zoomed in on Motorcycle 'A' and Vehicle 'B' bins.

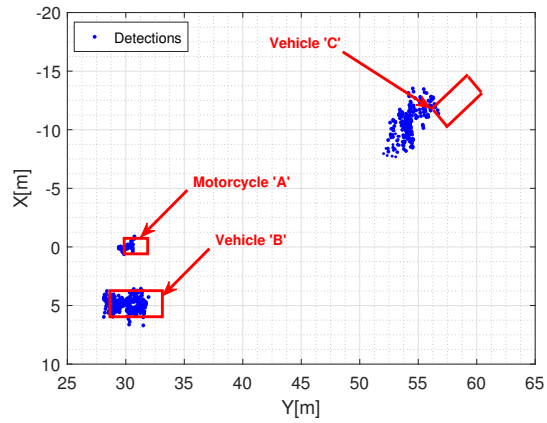

Fig. 7. Detection points in cartesian plane for integration time of 300msec. Red boxes mark the approximate the true object position.

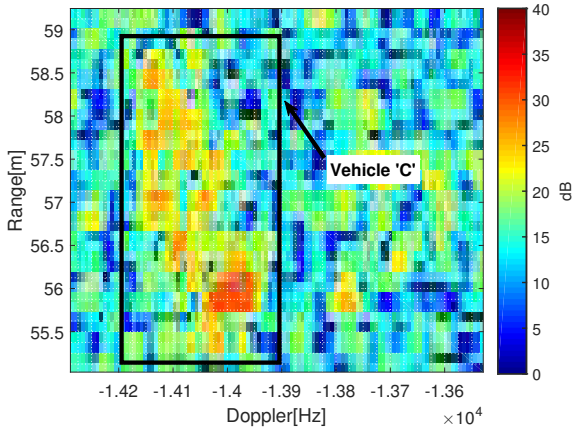

Fig. 9. Range-Doppler spectrum obtained for integration time of 50msec, zoom in on vehicle 'C bins.

of the scene causes the targets to have very close Doppler frequencies (but separable), due to the high Doppler resolution. Fig. 6 shows a segment of the range-Doppler spectrum focused around vehicle 'C'. It's spectrum is spread over many range-Doppler bins since the integration period is too long relative to the vehicles high speed and significant motion during that time window. Finally, in Fig. 7 we see the radar detections points (in a Cartesian plane) obtained from the 300 msec Doppler processing. The approximate ground truth positions are also plotted as red rectangles. Since the targets are moving during the integration time their detections are smeared across the (X,Y) plane in proportion to their relative velocity. This effect is negligible for Motorcycle 'A' and Vehicle 'B' since their relative velocity is low. Moreover, we see that due to the high Doppler resolution 'A' and 'B' are separable even though their angular spacing is *below* the radar angular resolution. On the other hand, the detections of vehicle 'C' were smeared and have a noticeable offset from the ground truth position.

Figs. 8-10 show the results obtained for processing the samples with 50 msec Doppler integration time. Fig. 8 shows the range-Doppler spectrum of motorcycle 'A' and vehicle 'B'. With this short integration duration and geometry of the scene, the Doppler frequencies of both targets overlap and are inseparable. Fig. 9 shows the range-Doppler spectrum segment around vehicle 'C'. We see that it spreads less compared to Fig. 6 and has a more accurate range estimation. Fig. 10 shows the detection points (in Cartesian plane) obtained from processing the samples with the short integration time. Contrary to Fig. 7, Motorcycle 'A' and vehicle 'B' are not separable due to the lower Doppler resolution, however, for vehicle 'C', the detection performance improved compared to Fig. 7 because it moved less during the short integration time.

The results in Figs. 5-10 demonstrates the fundamental tradeoff that is apparent in conventional Doppler processing with fixed integration time. The longer the integration duration, we obtain better target discrimination for low velocity targets but impair the position accuracy of high relative velocity targets. On the other hand, for short integration time we obtain better accuracy of the high speed target positions, but impair the ability to separate close objects. This tradeoff is resolved by multi-resolution Doppler processing as shown next.

Figs. 11-13 depict the results for the proposed multi-resolution Doppler processing method with the integration times given in Fig.2. Fig. 11 show the range-Doppler spectrum

ISBN 978-0-9928626-7-1 © EURASIP 2017

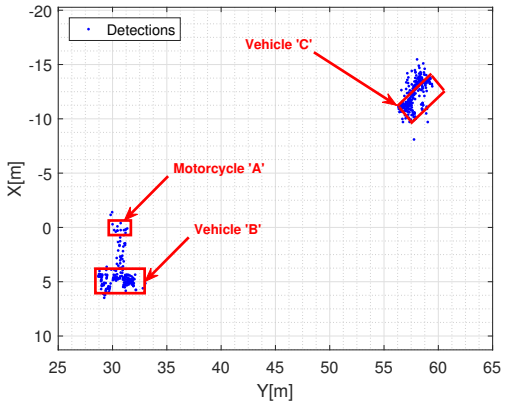

Fig. 10. Detection points in cartesian plane for integration time of 50 msec. Red boxes mark the approximate the true object position.

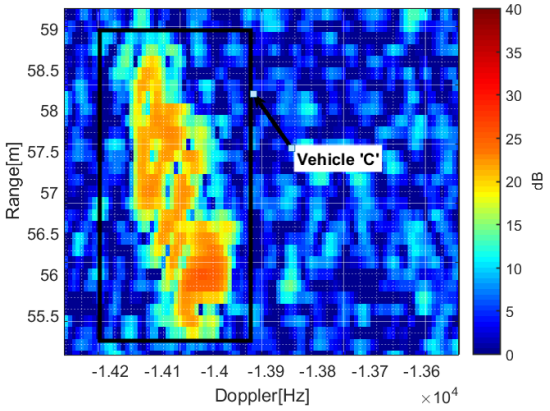

Fig. 12. Range-Doppler spectrum of the proposed method, zoomed in on around vehicle 'C'.

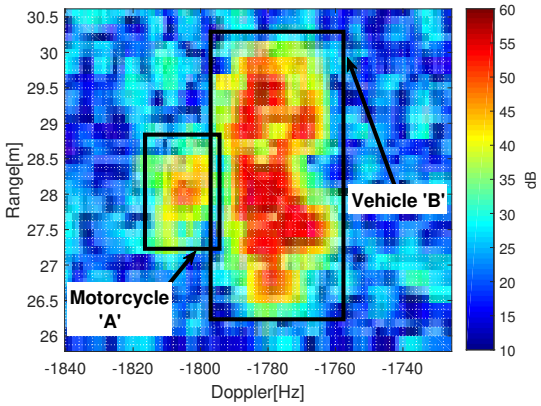

Fig. 11. Range-Doppler spectrum obtained of the proposed method, zoomed in on Motorcycle 'A' and vehicle 'B'.

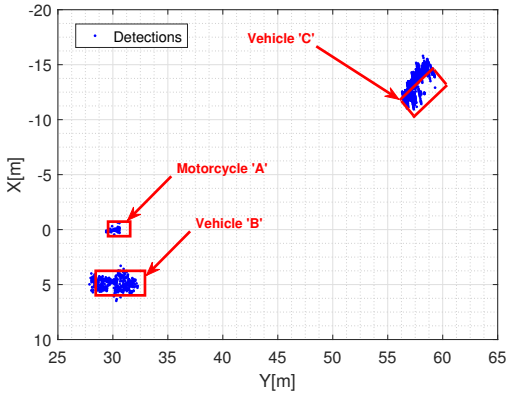

Fig. 13. Detection points in cartesian plane for the proposed method. Red rectangles depict the approximated ground truth.

around Motorcycle 'A' and vehicle 'B'. It is similar to Fig. 5. Targets have low Doppler frequency, thus, selected integration time for them is approximately 290msec, which yields high Doppler resolution and separates them. Fig. 12 shows the range-Doppler spectrum around vehicle 'C'. Selected integration time for this object was 37msec, thus, the vehicle's position does not change much during that period and the range estimation is more accurate and less smeared compared to Fig. 6. Lastly, Fig. 13 presents the radar detections derived from the multi-resolution method. It is apparent that the multi-resolution method attains more accurate detections relative to the fixed Doppler processing shown in Fig. 10 and Fig. 7.

V. Conclusions

A multi-resolution Doppler filtering method for automotive radar was developed. It was shown that it can resolve the fundamental tradeoff between high Doppler resolution that enables separation of close targets and the accuracy of the target position estimation. The performance advantage compared to conventional processing with fixed Doppler filtering resolution was demonstrated in an automotive radar scenario. The multi-resolution method achieved better object discrimination as well as better position estimation accuracy, which are both critical for automotive radar applications.

References

[1] H. Bloecher, J. Dickmann, and M. Andres, "Automotive active safety and comfort functions using radar," *IEEE International Conference on Ultra-Wideband*, pp. 490-494, IEEE, 2009.

[2] Continental, "ARS 408-21 Premium Long Range Radar Sensor 77 GHz", Available online: http://www.conti-online.com/www/download/industrial_sensors_de_en/themes/download/ars_premium_datenblatt_en.pdf

[3] Continental, "ARS 30X /-2 /-2C/-2T/-21 Long Range Radar", Available online: http://www.conti-online.com/www/download/industrial_sensors_de_en/themes/download/ars_300_datasheet_en.pdf

[4] Bosch, "LRR3: 3rd generation Long-Range Radar Sensor", Available online: http://products.bosch-mobility-solutions.com/media/db_application/pdf_2/en/lrr3_datenblatt_de_2009.pdf

[5] B. R. Mahafza*Radar Systems Analysis and Design Using MATLAB*, Chapter 3, CRC Press, Inc. ,2000

[6] A. Wojtkiewicz, J. Misiurewicz, M. Nalecz, K. J. drzejewski, K. Kulpa, "Two-dimensional signal processing in FMCW radars," *Proceedings of the XX-th National Conference Circuit Theory and Electronic Networks*, vol 2, Oct. 1997

[7] V. Winkler, "Range Doppler detection for automotive FMCW radars," *2007 European Microwave Conference*, Oct 2007.

[8] M. Song, J. Lim, and D.-J. Shin, "The velocity and range detection using the 2D-FFT scheme for automotive radars," *2014 4th IEEE International Conference on Network Infrastructure and Digital Content*, Sept. 2014.

[9] M. A. Richards *Fundamentals of Radar Signal Processing*, McGraw-Hill, 2005.

[10] H. Rohling, "Radar CFAR Thresholding in clutter and multiple target situations," *IEEE Transactions on Aerospace and Electronic Systems*, vol. AES-19, no. 4, pp. 608-621, Jul. 1983.

ISBN 978-0-9928626-7-1 © EURASIP 2017